Condensation of a Zeotropic Refrigerant R-32/R-125/R-134a (23%/25%/52%) in a Horizontal Tube

P. J. Kenney, J. C. Chato, M. K. Dobson, J. P. Wattelet, J. A. Gaibel,
M. Ponchner, R. L. Shimon, T. C. Villaneuva, N. L. Rhines, K. A. Sweeney,
D. G. Allen, and T. T. Hershberger

ACRC TR-62 July 1994

For additional information:

Air Conditioning and Refrigeration Center
University of Illinois
Mechanical & Industrial Engineering Dept.
1206 West Green Street
Urbana, IL 61801

(217) 333-3115

Prepared as part of ACRC Project 37
Effect of Geometric Variables and R-22 Alternatives on Refrigerant-Side Evaporation and Condensation
J. C. Chato, Principal Investigator

The Air Conditioning and Refrigeration Center was founded in 1988 with a grant from the estate of Richard W. Kritzer, the founder of Peerless of America Inc. A State of Illinois Technology Challenge Grant helped build the laboratory facilities. The ACRC receives continuing support from the Richard W. Kritzer Endowment and the National Science Foundation. The following organizations have also become sponsors of the Center.

Acustar Division of Chrysler
Allied-Signal, Inc.
Amana Refrigeration, Inc.
Brazeway, Inc.
Carrier Corporation
Caterpillar, Inc.
E. I. du Pont de Nemours & Co.
Electric Power Research Institute
Ford Motor Company
Frigidaire Company
General Electric Company
Harrison Division of GM
ICI Americas, Inc.
Modine Manufacturing Co.
Peerless of America, Inc.
Environmental Protection Agency
U. S. Army CERL
Whirlpool Corporation

For additional information:

Air Conditioning & Refrigeration Center
Mechanical & Industrial Engineering Dept.
University of Illinois
1206 West Green Street
Urbana IL 61801

217 333 3115

ABSTRACT

This experimental study examined the local heat transfer coefficients and frictional pressure gradients of a ternary zeotropic refrigerant mixture, R-32/R-125/R-134a (23%/25%/52%) condensing in a smooth, horizontal tube. The test section consisted of a 3 ft long, copper tube with a diameter of 0.277 in (7.04 mm) surrounded by a counter-flow, water-cooled annulus. Test conditions varied the average quality from 10% to 90% and the mass flux from 55 to 474 klb/ft^2-hr (75 to 650 kg/m^2-s) to insure that data points were taken all across the wavy and annular flow regimes. The temperature difference was held approximately constant at 5.4 °F (3.0 °C). At mass fluxes higher than 364 klb/ft^2-hr (500 kg/m^2-s), the Dobson correlation consistently overpredicted the heat transfer coefficients requiring a least squares-determined factor of 0.836 to correct. As the flow regime approached wavy flow, the Dobson correlation increasingly overpredicted the heat transfer coefficient due to the dominance of zeotropic degradation. Frictional pressure gradient data showed similar trends to the Souza pressure drop correlation but were significantly lower.

TABLE OF CONTENTS

LIST OF TABLES

Tables

LIST OF FIGURES

Figures

NOMENCLATURE

Symbols		Definitions
c	constant	
c_p	specific heat at constant pressure	
D	diameter	
f_l	liquid friction factor for smooth tubes	$\frac{0.079}{Re_l^{0.25}}$
Fr_l	liquid only Froude number	$\frac{G^2}{\rho_l^2 g D}$
Fr_{so}	Soliman's modified Froude number	Eq. (2.8)
g	acceleration due to gravity	
$g_{effective}$	effective gravity term	Eq. (2.14)
G	mass flux	
Ga	Galileo number	$\frac{\rho_l(\rho_l - \rho_v)D^3}{\mu_l^2}$
h	heat transfer coefficient if unsubscripted, enthalpy if subscripted	
h_{fg}	heat of vaporization	
Ja	Jakob number	$\frac{c_{p_l}(T_{sat} - T_{wall})}{h_{fg}}$
k	thermal conductivity	
L	test section length	
$\dot{m}$	mass flow	
Nu	Nusselt number	$\frac{hk}{D}$
Ph	Phase change number	Eq. (2.4)
P	pressure	
Δp	pressure drop	
Pr	Prandtl number	$\frac{\mu c_p}{k}$
$\left(\frac{\Delta p}{\Delta z}\right)$	pressure gradient	
q"	heat flux	
$\dot{q}$	rate of heat transfer	
$\dot{q}_{loss}$	heat loss to the environment	
R	a density/viscosity ratio	Eq. (2.6)

Re	Reynolds number	$\frac{GD}{\mu}$
Re_{eq}	equivalent Reynolds number	Eq. (2.2)
Re_L	Reynolds number based on length	Eq. (2.5)
Re_l	superficial liquid Reynolds number	$\frac{G(1-x)D}{\mu_l}$
Re_v	superficial vapor Reynolds number	$\frac{GxD}{\mu_v}$
Re_{vo}	vapor-only Reynolds number	$\frac{GD}{\mu_v}$
T	temperature	
$\overline{T}$	average temperature	
U	velocity	
UA	overall heat transfer coefficient	
x	quality	
X	Lockhart-Martinelli parameter	Eq. (2.21)
X_{tt}	turbulent-turbulent Lockhart-Martinelli parameter	Eq. (2.12)
$f = f\{\ \}$	function, parentheses enclose independent variable(s)	

Greek		Definitions
α	void fraction	Eq. (2.20)
δ	uncertainty in a measurement	
ϕ_l	two-phase multiplier	Eq. (2.22)
ρ	density	
μ	viscosity	

subscripts	
a	air
avg	average
b	boiler
f	frictional
i	inner
in	inlet of component
l, liquid	liquid
liq	saturated liquid
out	outlet of component
s	surface
sat	saturated conditions
ts	test section
v, vapor	vapor
vap	saturated vapor
w	water
wall	tube wall
∞	fluid

CHAPTER 1
Introduction

The basis of this research is an extension of the first project of the Air Conditioning and Refrigeration Center at the University of Illinois, Urbana-Champaign. Begun in 1989, the purpose of this initial endeavor was to explore two-phase heat transfer in horizontal tubes and to create a foundation of knowledge in order to evaluate alternative refrigerants. The project was divided into two separate facilities; one dedicated to the studies of evaporation, and another to condensation. The capstone for this foundational research has been completed by Wattelet (1994) and Dobson (1994) for evaporation and condensation, respectively.

The impetus for the generation of this project and the Center has been the general concern for the environmental impact of refrigerants and the conservation of energy. Regulations have been created that call for the eventual phase-out of man-made chlorofluorocarbons (CFCs) and hydrochlorofluorocarbons (HCFCs). In addition, standards for higher efficiencies in refrigerant-using appliances were mandated. As a result, affected industries seek alternative refrigerants.

One possibility of the alternative refrigerant is a zeotropic mixture of refrigerants. A zeotrope possesses the distinguishing characteristic of a temperature glide as the mixture changes phase at constant pressure. The more volatile component vaporizes preferentially in the condition of two-phase.

To engineer a cycle, one needs heat transfer coefficient and pressure drop information. The present study examines the condensation of a ternary zeotrope that interests industry: R-32/R-125/R-134a (23%/25%/52%). This potential alternative possesses a temperature glide of 9 °F (5 °C) at typical condensing temperatures.

Chapter 2 contains a review of literature on internal, horizontal tube condensation of zeotropes. Also, a summarizing background is presented of Dobson's foundational knowledge of condensation. In chapter 3, the experimental facility and data analysis are described. The results of the heat transfer coefficient and pressure drop are examined in chapter 4 with comparisons to current correlations. Chapter 5 concludes the thesis with a summary of the findings and recommendations for further work.

CHAPTER 2
Literature Review

This chapter presents not only a literature review of publications on zeotropic refrigerants but also background information on condensation. In many of the sources zeotropes are referred to as nonazeotropic refrigerants or blends (NARMs or NARBs). This cumbersome title has been shortened to zeotropic refrigerants or just zeotropes in this thesis. The background on condensation includes a review of flow regimes, a current heat transfer coefficient correlation, and a correlation for two-phase, frictional pressure drop.

2.1 Zeotropes

Experimental data of heat transfer coefficients for zeotropic refrigerants condensing in horizontal tubes are sparse. In Wang and Chato's (1992) review of recent research in zeotropic condensation, only a little more than a dozen sources offer insight into zeotropic forced convection. A shortcoming of some of the zeotropic research is the lack of a common, comparative base.

One publication compared zeotrope data to a pure refrigerant correlation. Bivens and Yokozeki (1992) found good agreement between Eckels and Pate's (1991) ternary zeotrope, R-124/R-22/R-152a (40%/36%/24%), data and Cavellini and Zecchin's (1974) heat transfer coefficient correlation. This correlation assumes annular flow for its two-phase multiplier form.

$$Nu = 0.05\,Re_{eq}^{0.8}\,Pr_l^{0.33} \tag{2.1}$$

$$Re_{eq} = Re_l + Re_v \frac{\mu_v}{\mu_l}\left(\frac{\rho_l}{\rho_v}\right)^{0.5} \tag{2.2}$$

Koyama (1988) compares the zeotropic data of R-22/R-114 to an empirical correlation developed by Fujii and Nagata (1973). The flow regimes of the data are reported to be annular and semi-annular. Using the correlation presented in Equation (2.3) the zeotrope was overpredicted by a maximum of 20%. A phase change number, Ph, is defined in Equation (2.4) for use in the correlation. Notice that the Reynolds number deviates from standard definitions for internal condensation. Stoecker and Kornata (1985) also noticed a reduction in the heat transfer coefficient when they studied R-22/R-114.

$$Nu = 0.25\left(\frac{D_i}{L}\right)^{0.4} Ph^{-0.6}\left(\frac{Re_L\,Pr_l}{R}\right)^{0.8} \tag{2.3}$$

$$Ph = \frac{c_{p_l}\left(T_{sat} - \overline{T}_{wall}\right)}{h_{sat,vapor,in} - h_{sat,liquid,out}} \tag{2.4}$$

$$Re_L = \frac{\rho_l U_v L}{\mu_l} \tag{2.5}$$

$$R = \left(\frac{\rho_l \mu_l}{\rho_v \mu_v}\right)^{0.5} \tag{2.6}$$

In 1980, Bokhanovskiy tested various compositions of a zeotropic mixture of R-12 and R-22. His results were more qualitative in nature, because he compared the heat transfer coefficients to one another. He concluded that there is a reduction in heat transfer coefficient due to the diffusion resistance when the heat flux is less than 5700 Btu/h-ft^2 (18 kW/m^2).

Mochizuki (1988, 1990) and Inoue (1988) compared binary zeotropes of R-113/R-11 and R-113/R-114 to their pure components. At high Reynolds numbers, which infers the annular flow regime, the R-113/R-11 mixture's heat transfer coefficients were between those of its components. However, at all mass fluxes the R-113/R-114 zeotrope produced smaller heat transfer coefficients than those of both R-113 and R-114.

In all of this experimental research, not one source finds any improvement in the heat transfer coefficient using zeotropic refrigerants. At best, a mixture's heat transfer coefficient was found between its two components. Also, there is some discrepancy among the publications whether an annular flow correlation can correctly predict the Nusselt number. However, with a variety of tested zeotropes, one could easily speculate that this predictive ability is based on the interactions among components and the mixture's composition.

Koyama (1988) corrected his annular correlation with a third-order polynomial based on one of the two component's mass fraction. Although this method works well for this particular refrigerant, it sheds no insight on a method applicable to all zeotropes.

2.2 Flow Regimes

The characterizations of flow regimes are important in condensation, because they control the mechanism of heat transfer that is occurring. Two independent variables drive the characterization of flow regimes: quality and mass flux. The latter term can be split into superficial mass fluxes for both the vapor and liquid phases, because the relative velocity between the two phases is the important value. Due to transition regimes and methods of

viewing, flow regimes are fairly subjective in nature; however, there exist two extreme flow types with which to begin.

In a horizontal tube, wavy flow designates a complete stratification of phases due to the force of gravity. Other gravity-driven flow regime classifications include stratified flow and intermittent flow. Stratified flow is a broad term used to indicate phase separation and is typically coupled with a modifier of wavy or smooth. In stratified-wavy flow, the vapor phase has a velocity greater than that of the liquid causing Helmholtz instability at the vapor-liquid interface. One can deduce that stratified-smooth classifies flow that has not reached this instability state. Intermittent flow is characterized by stratified flow sections separated by completely liquid plugs. This regime can develop from a smooth regime at much lower qualities and from a wavy regime when the crests of the waves reach the top of the tube. Since stratified-wavy flow dominates these data, wavy flow will characterize all of the gravity-driven regimes.

As the vapor velocity increases relative to the liquid velocity, another flow regime begins to develop: annular flow. This regime is characterized by a uniform layer of liquid around the perimeter of the tube with a core of vapor where shear forces between the two phases dominate gravity. The exact location of this regime is very difficult to pinpoint. Even with a sight glass, the turbulence in the liquid layer inhibits clear viewing.

A transition regime that is described as annular flow with a thickened liquid layer at the bottom of the tube is encountered quite frequently during testing. There is a great deal of subjectivity in the designation of this flow. In this research, a regime of wavy-annular denotes this transition flow.

2.3 Annular Flow Correlation

Within annular flow, forced convection exclusively dominates the mechanism of heat transfer as in single phase; vapor shear forces create increased pressure drop but also increased heat transfer coefficient. There are several techniques that one can use to model the heat transfer coefficient for annular flow. The more theoretical solutions develop correlations from an analysis of the thin liquid, boundary layer or from the shear forces directly. The simplest method bases the correlation upon a two-phase multiplier and a single-phase correlation such as Dittus-Boelter's [Incropera and DeWitt (1992)].

$$Nu = 0.023 Re_l^{0.8} Pr_l^{0.4} \tag{2.7}$$

The most recent correlations that attempt to predict the heat transfer coefficient for condensation at every flow condition are Dobson's (1994). The boundaries that separate the two distinct equations attempt to quantitatively distinguish between annular flow and the

transition between annular and wavy-annular flows. Dobson (1993) found that a Froude number, defined by Soliman (1968) and shown in Equations (2.8), (2.9), and(2.10), greater than 20 was a good predictor of annular flow. In 1994, he found that at and above a mass flux of 364 klb/ft^2-hr (500 kg/m^2-s) the heat transfer coefficient can be exclusively predicted by his annular correlation independently of Froude number.

$$Fr_{so} = c_1 \, Re_l^{c_2} \, Ga^{-0.5} \left(\frac{1 + X_{tt}^{0.039}}{X_{tt}} \right) \tag{2.8}$$

For $Re_l < 1250$

$$c_1 = 0.025 \tag{2.9a}$$

$$c_2 = 1.59 \tag{2.9b}$$

For $Re_l \geq 1250$

$$c_1 = 1.26 \tag{2.10a}$$

$$c_2 = 1.04 \tag{2.10b}$$

In the development of his correlation, Dobson (1994) justified the use of a two-phase multiplier correlation through a rigorous analysis of the highly theoretical Traviss (1973) analysis. He selected this particular form of the multiplier for its success as a single-phase predictor and its ability to collapse to the Dittus-Boelter solution as quality goes to zero. Equation (2.11) shows the annular flow correlation.

$$Nu = 0.023 \, Re_l^{0.8} \, Pr_l^{0.4} \left[1 + \frac{2.22}{X_{tt}^{0.889}} \right] \tag{2.11}$$

The variable in the two-phase multiplier is the turbulent-turbulent variation of the Lockhart and Martinelli (1947) parameter defined:

$$X_{tt} = \left(\frac{\rho_v}{\rho_l} \right)^{0.5} \left(\frac{\mu_l}{\mu_v} \right)^{0.1} \left(\frac{1 - x}{x} \right)^{0.9} \tag{2.12}$$

2.3 Wavy Flow Correlation

The mechanism of heat transfer for gravity-driven regimes is primarily due to conduction through the liquid film between the vapor phase and the tube. This process for internal condensation was modeled by Chato (1962) who developed a correlation for heat transfer coefficient deriving from Nusselt's (1916) analysis of a falling film on a vertical plate. Chato hypothesized that the heat transfer across a gravity-driven laminar layer

developing at the top of the tube and running down the tube wall to the liquid phase completely dominates the total two-phase heat transfer. Therefore, his correlation is solely conduction-based and neglects heat transfer from the liquid phase at the bottom of the tube.

Dobson (1994) developed a correlation for the wavy flow regime that includes a conduction-based term but also a forced convection based term. This effectively extends the usable range of this correlation into the transition region between wavy flow and the shear force dominated annular flow. From the previously presented boundaries, one can deduce that the usable range for this composite equation is where the mass flux is below 364 klb/ft^2-hr (500 kg/m^2-s) and the Froude number is below 20.

$$Nu = Nu_{film} + Nu_{forced} \tag{2.13}$$

The filmwise term borrows an effective gravity component from external condensation analysis completed by Dhir and Lienhard (1971) for horizontal tubes. Also, the numerical coefficients are selected to collapse this term to a heat transfer coefficient correlation for external condensation, which is shown in Equation (2.14), as quality approaches zero.

$$Nu_{external} = 0.728\underbrace{\left[\frac{Ga\,Pr_l}{Ja}\right]^{0.25}}_{g_{effective}} \tag{2.14}$$

The power law relation of the vapor only Reynolds number was suggested by Rosson and Myers (1965) in their internal condensation analysis. To account for quality and refrigerant property dependencies, the Lockhart-Martinelli parameter was again included.

$$Nu_{film} = \frac{0.23Re_{vo}^{0.12}}{1+1.11X_{tt}^{0.58}}\underbrace{\left[\frac{Ga\,Pr_l}{Ja}\right]^{0.25}}_{g_{effective}} \tag{2.15}$$

As one would expect, the forced convection term, Equation (2.16), is similar to the annular flow correlation; however, it uses a more conservative two-phase multiplier. This multiplier is drawn from Souza's (1992) pressure drop correlation that was developed from evaporation data and is shown in Equation (2.17) with coefficients defined in Equations (2.18) and (2.19).

Since this term is secondary and exists to extend the range into the transition regime, a weighting function must be included. Weighting is dependent on the hydraulic diameter of the liquid phase [Taitel and Dukler (1976)]; although, this is not easily quantified. Jaster and Kosky (1976) reformulated this diameter dependence to be based on void fraction; however, since there is a transcendental component, the weighting function is

only a close approximate relation. The void fraction, which is shown in Equation (2.20), is that of Zivi's definition (1964) at minimum entropy generation.

$$Nu_{forced} = \left[\frac{\arccos(2\alpha - 1)}{\pi}\right] 0.0195 Re_l^{0.8} Pr_l^{0.4} \phi_l(X_{tt}) \tag{2.16}$$

$$\phi_l(X_{tt}) = \sqrt{1.376 + \frac{c_1}{X_{tt}^{c_2}}} \tag{2.17}$$

For $0 < Fr_l \leq 0.7$

$$c_1 = 4.172 + 5.48 Fr_l - 1.564 Fr_l^2 \tag{2.18a}$$

$$c_2 = 1.773 - 0.169 Fr_l \tag{2.18b}$$

For $Fr_l > 0.7$

$$c_1 = 7.242 \tag{2.19a}$$

$$c_2 = 1.655 \tag{2.19b}$$

$$\alpha = \left[1 + \frac{1-x}{x}\left(\frac{\rho_v}{\rho_l}\right)^{2/3}\right]^{-1} \tag{2.20}$$

2.4 Pressure Drop Correlation

Total pressure drop is comprised of three components due to separate forces: friction, acceleration, and gravity. In horizontal tubes, pressure drop due to gravity forces is nonexistent. Acceleration pressure drop is due to the momentum change as the fluid changes phases and can be calculated using the void fraction. In these data, pressure drop due to acceleration is small. The remaining pressure drop that is generated from frictional forces is computed using a two-phase multiplier or friction factor.

Lockhart and Martinelli (1947) first suggested that these multiplier terms be based on the ratio of the pressure gradient due of liquid phase to the vapor phase. They included several parameters based on whether the phases are either turbulent or laminar. The most popular combination is the turbulent-turbulent case shown previously in Equation (2.12).

$$X^2 = \frac{\left(\frac{\Delta p}{\Delta z}\right)_l}{\left(\frac{\Delta p}{\Delta z}\right)_v} \tag{2.21}$$

The two-phase multiplier used in the forced convection term of the wavy flow correlation is shown in Equation (2.22) as the ratio of actual pressure gradient to the pressure gradient generated by the liquid phase.

$$\phi_l^2 = \frac{\left(\frac{\Delta p}{\Delta z}\right)_f}{\left(\frac{\Delta p}{\Delta z}\right)_l} \tag{2.22}$$

Souza's (1992) correlation of this two-phase multiplier is shown in Equation (2.17) with coefficients defined in Equations (2.18) and (2.19). Frictional pressure drop can be predicted using this correlation in Equation (2.23). The friction factor used for this analysis is shown in Equation (2.24).

$$\left(\frac{\Delta p}{\Delta z}\right)_f = \left(\frac{\Delta p}{\Delta z}\right)_l \phi_l^2 = -\left(\frac{2 f_l G^2 (1-x)^2}{\rho_l D}\right)\phi_l^2 \tag{2.23}$$

$$f_l = \frac{0.079}{Re_l^{0.25}} \tag{2.24}$$

CHAPTER 3

Experimental Facility and Data Analysis

This chapter describes the experimental facility, test conditions, and data analysis techniques. A detailed account of the fabrication of the current apparatus was discussed by Gaibel (1994) with its evolution accounted in Dobson (1994), Hinde (1992), and Bonhomme (1991). This thesis reviews the equipment and touches on the important components; Figure 3.1 shows the schematic of the facility. Measurement uncertainties are included as background for the uncertainty analysis of the data results. Detailed operational procedures are identical to Gaibel (1994) and are omitted; however, the test conditions are included with reasoning for their selection. Within the data collection section, calculations of important data results are presented with an uncertainty analysis. Appendix A tabulates property curve-fits for the ternary refrigerant zeotrope.

3.1 Experimental Facility

This section contains a brief overview of the facility. First, the test section and its instrumentation are discussed. Second, the surrounding facility that is used to set testing conditions is reviewed.

3.1.1 Test Section

The test section is a counter-flow, annular water-cooled condenser. The smooth, horizontal copper tube includes a diabatic section which has a plastic annulus approximately 3 ft long and an adiabatic section 2 ft long which precedes the condensing section. Sight glasses are mounted immediately preceding and following the test condenser to allow visual observation of the flow regime. The entire refrigerant tube has an inner diameter of 0.277 in (7.04 mm).

The refrigerant, wall, and water temperature measurements are produced by copper-constantan, type T thermocouples which are referenced to an ice-bath. The refrigerant and wall thermocouples are soldered into grooves in the wall. The former are measured at the top and bottom of the tube at inlet and outlet adiabatic sections; the latter are in four locations around the tube at 60° increments because a vertically symmetrical temperature profile is assumed. These temperature readings are averaged and weighted by their respective perimeter. The water thermocouples are probes located within the turbulent flow; the well-mixed water is fairly uniform in temperature.

The two inlet absolute pressure transducers possess more than triple their calibrated uncertainty due to day to day drifting. Since the outlet transducer has a much larger range and uncertainty, it was only used during leak searches. Instead, a differential pressure transducer measurement across the diabatic section is added to the inlet absolute pressure measurement to calculate the outlet pressure. To isolate the frictional pressure gradient, pressure drop is measured across the adiabatic section. Table 3.1 summarizes the individual devices' uncertainties in the order in which they are described.

Table 3.1 Test section measurement uncertainty summary

Measurement Device	Uncertainty
Refrigerant Thermocouples	±0.36 °F (±0.2 °C)
Wall Thermocouples	±0.36 °F (±0.2 °C)
Water Thermocouples	±0.18 °F (±0.1 °C)
Inlet Absolute Pressure Transducers	±1 psia (±7 kPa)
Outlet Absolute Pressure Transducer	±5 psia (±35 kPa)
Differential Pressure Transducers	±0.03 psia (±0.2 kPa)

3.1.2 Standing Apparatus

Refrigerant is circulated by a positive-displacement gear pump. By not using a compressor, the refrigerant loop avoids oil contamination and maintains a single operating pressure. The lowest mass flux, 55 klb/ft^2-hr (75 kg/m^2-s), through 220 klb/ft^2-hr (300 kg/m^2-s) is measured using a coriolis-effect, mass flow meter. The higher mass fluxes, 364 klb/ft^2-hr (500 kg/m^2-s) and 474 klb/ft^2-hr (650 kg/m^2-s), are determined by a positive-displacement, volumetric flow meter. Water mass flow is determined using a graduated cylinder and stopwatch.

The boiler is serpentine in configuration with 20 electric heater tapes attached to a 0.375 in. outer diameter, copper tube. A Variac controls 10 heaters while another 10 heaters are individually switched on and off. The maximum power deliverable to the refrigerant is 6.4 kW. The power input is measured by watt-hour power transducers. Heat that is not removed by the test condenser is removed by a water-cooled aftercondenser and a water-cooled subcooler, in order to assure that subcooled liquid reaches the pump.

Apparatus pressure is controlled by immersing a large container, that is assured of containing a two-phase mixture of refrigerant, within a constant temperature bath. The water bath is heater controlled with a small mixer. The large thermal inertia of the bath

insures stable pressure within the system. Table 3.2 summarizes the measurement devices with their respective uncertainties in the order in which they are described.

Table 3.2 Apparatus measurement uncertainty summary

Measurement Device	Uncertainty
Mass Flow Meter	±0.1 % of reading
Volumetric Flow Meter	±1.4 L/s
Heater Power Transducers	±0.2 % of reading
Boiler Inlet Thermocouple	±0.54 °F (±0.3 °C)
Boiler Inlet Absolute Pressure Transducer	±5 psia (±35 kPa)

3.2 Test Conditions

The purpose for the development of this research apparatus was to provide data on the heat transfer of condensation by alternative refrigerants. Since the primary use of refrigerants is in refrigeration units and air conditioners, test conditions must span the ranges of these operating systems. The range of mass flow is large between systems, because it can vary by two magnitudes from domestic refrigerators to automobile air conditioners. The range of mass flux test conditions was chosen to develop wavy flow at the lower mass fluxes and annular flow at the higher fluxes. It also allows for the investigation of the transition regime. The tested mass fluxes were 55, 110, 220, 364, and 474 klb/ft^2-hr (75, 150, 300, 500, and 650 kg/m^2-s).

Saturation temperature was selected to be 95 °F (35 °C) for three reasons. First, it lies within the range of actual operating systems, although at the low end. Second, heat transfer is not dependent on the fluid temperature, but the temperature difference between the exchanging fluids. Last, by operating near the ambient air temperature, heat loss to the environment within each component can be minimized.

Since the data acquisition system calculates an average heat transfer coefficient, data points are taken at various average qualities. The test condenser typically removes heat from the refrigerant to change the quality between 25% to 5%; therefore, the inlet quality can range from 95% to as low as 10%, as long as the outlet is two-phase. Thus, average qualities range from 90% to approximately 7%.

The last condition that can be regulated is the temperature difference between the refrigerant and the wall. Dobson (1994) showed that this temperature difference directly affects heat transfer within the wavy flow regime. Therefore, to avoid any variation in the testing, this value was held approximately constant at 5.4 °F (3 °C).

3.3 Data Analysis

This section details the reduction of the data into a local heat transfer coefficient and an average quality. Their calculation is detailed and followed by the equations of each necessary variable. An uncertainty analysis is included at the end of this section.

3.3.1 Heat Transfer Coefficient Calculation

The heat transfer coefficient is defined using Newton's law of cooling and shown as Equation (3.1). The determined value is an average over a small quality range. When compared to other average values, the data can be correlated to predict local heat transfer coefficients.

$$h = \frac{q''}{(T_\infty - T_s)} \tag{3.1}$$

Heat flux is determined from the rate of heat transferred to the water and to the environment divided by the tube's inside surface area. The water's heat transfer rate is calculated using Equation (3.2) where the mass flow and temperatures are measured and the specific heat is determined by a curve fit using the average of the water temperatures.

$$\dot{q}_w = \dot{m}_w c_{p_w} (T_{out} - T_{in})_w \tag{3.2}$$

Heat loss to the environment is calculated using an overall heat transfer coefficient. Dobson (1994) determined this characteristic by using various single phase tests. Equation (3.3) shows the calculation.

$$\dot{q}_{loss,ts} = UA_{ts}\left(\left(\frac{T_{in} + T_{out}}{2}\right)_w - T_a\right) \tag{3.3}$$

The fluid temperature corresponds to the saturation temperature of the refrigerant. With the temperature glide of zeotropes, the actual saturation temperature can be somewhat elusive. For these tests, the glide temperatures are based on the average of the inlet and outlet pressures; they are different due to pressure drop. The saturation temperature is linearly interpolated between the vapor-liquid temperature glide based on the average quality.

$$T_{sat} = T_{liq} + x_{avg}(T_{vap} - T_{liq}) \tag{3.4}$$

$$T_{liq} = T_{sat,liquid}\left\{P_{ts,in} - \frac{\Delta p_{ts}}{2}\right\} \tag{3.5}$$

$$T_{vap} = T_{sat,vapor}\left\{P_{ts,in} - \frac{\Delta p_{ts}}{2}\right\} \tag{3.6}$$

Surface temperature is simply the average of the wall thermocouples. With the surface area being a function of inner diameter and length, the heat transfer coefficient is expressed as Equation (3.7).

$$h = \frac{\dot{q}_w + \dot{q}_{loss,ts}}{\pi D_i L\left(T_{sat} - \overline{T}_{wall}\right)} \tag{3.7}$$

3.3.2 Quality Calculation

To calculate the quality, a control volume is drawn around the boiler, and the first variable that must be determined is inlet enthalpy. The subcooled refrigerant's enthalpy that enters the boiler is determined from Equation (3.8). The fluid enthalpy and density are calculated from property curve fits of the saturated liquid using a pressure that is based on the inlet to the boiler temperature. The pressure difference between the inlet and the outlet of the boiler is used to determine the subcooled work energy, because the saturation pressure at this state point is that of the boiler outlet. Although this method neglects pressure drop due to friction and acceleration within the boiler, it approximates the subcooled enthalpy well.

$$h_{b,in} = h_{liq} + \frac{\left(P_{b,in} - P_{sat}\right)}{\rho_{liq}} \tag{3.8}$$

$$h_{liq} = h_{sat,liquid}\left\{P_{b,in}\right\} \tag{3.9}$$

$$\rho_{liq} = \rho_{sat,liquid}\left\{P_{b,in}\right\} \tag{3.10}$$

$$P_{sat} = P_{b,out} \tag{3.11}$$

Heat gain from the heaters is added to the refrigerant to calculate the outlet enthalpy; however, heat loss exists to the environment within the insulated boiler. As in the test section, a characteristic overall heat transfer coefficient was derived by Dobson (1994) using the difference between a weighted average of the inlet and outlet to the boiler temperatures and the ambient air temperature.

$$\dot{q}_{loss,b} = UA_b\left(\tfrac{3}{16}T_{b,in} + \tfrac{13}{16}T_{b,out} - T_a\right) \tag{3.12}$$

Therefore, using a control volume around the refrigerant-side of the boiler, the outlet enthalpy can be calculated from Equation (3.13). The heater power and refrigerant mass flow are direct measurements.

$$h_{b,out} = h_{b,in} + \frac{\left(\dot{q}_h - \dot{q}_{loss,b}\right)}{\dot{m}_r} \tag{3.13}$$

By definition, the quality entering the test section is calculated using the boiler's outlet enthalpy, the saturated liquid enthalpy, and the heat of vaporization where the latter two are based on property curve-fits using the test section's inlet pressure.

$$x_{in} = \frac{h_{b,out} - h_{liq,in}}{h_{fg,in}} \tag{3.14}$$

$$h_{liq,in} = h_{sat,liquid}\left\{P_{ts,in}\right\} \tag{3.15}$$

$$h_{fg,in} = h_{sat,fg}\left\{P_{ts,in}\right\} \tag{3.16}$$

The outlet quality includes the heat removed in the test section by the water and the accompanying heat loss. Also, the outlet pressure to the test section is used to calculate the liquid enthalpy and heat of vaporization.

$$h_{ts,out} = h_{b,out} - \frac{\left(\dot{q}_w + \dot{q}_{loss,ts}\right)}{\dot{m}_r} \tag{3.17}$$

$$x_{out} = \frac{h_{ts,out} - h_{sat,liquid}}{h_{sat,fg}} \tag{3.18}$$

$$h_{liq,out} = h_{sat,liquid}\left\{P_{ts,in} - \Delta p_{ts}\right\} \tag{3.19}$$

$$h_{fg,out} = h_{sat,fg}\left\{P_{ts,in} - \Delta p_{ts}\right\} \tag{3.20}$$

The reported quality of each test is an average to the test section's inlet and outlet qualities.

$$x_{avg} = \frac{x_{in} + x_{out}}{2} \tag{3.21}$$

3.3.3 Uncertainty Analysis

Dobson (1994) completed an extensive uncertainty analysis for a similar method of calculating the heat transfer coefficient and quality. He used the methods that were

described by Moffat (1988). Equation (3.22) summarizes this technique of estimating the uncertainty of a calculation from its independent variables' uncertainties.

$$\delta y = \sqrt{\sum_{i=1}^{N}\left(\frac{\partial y}{\partial x_i}\delta x_i\right)^2} \tag{3.22}$$

The present study deviates from Dobson's original heat transfer coefficient calculation in only one area: saturation temperature. With pure and azeotropic refrigerants, saturation temperature was determined from the measured inlet temperature to the test section. However, as has been discussed previously, the zeotropic temperature glide demands an alternative method for determining the saturation temperature which is shown in Equation (3.4). Notice that average quality appears in the equation; this presents some complications. While calculating the uncertainty of quality, one discovers that it is necessary to calculate the uncertainty of an 'independent variable,' enthalpy.

To avoid this problem, this analysis attempts to validate Dobson's uncertainty analysis by showing that the uncertainty of the present saturation temperature case is close to that of Dobson's original case. The uncertainty of the zeotropic saturation temperature uses Dobson's uncertainty of quality as a first guess.

$$\delta T_{sat} = \sqrt{\left((1-x_{avg})\delta T_{liq}\right)^2 + \left(x_{avg}\delta T_{vap}\right)^2 + \left((T_{vap}-T_{liq})\delta x_{avg}\right)^2} \tag{3.23}$$

The uncertainty of the two glide temperatures is determined by perturbing the property curve fits by the uncertainty of pressure. At typical operating pressures, this value is consistently around 0.34 °F (0.19 °C). Uncertainty in the average quality was taken from Dobson's worst case: 2%.

The uncertainty for the saturation temperature was calculated at the extreme test conditions of mass flux and quality. In each case, the temperature glide varies from 9.4 °F (5.2 °C) by no more than a few hundredths of a degree. Therefore, the range of the calculated uncertainty is from 0.337-0.364 °F (0.187-0.202 °C). Since this range is very near to the 0.36 °F (0.2 °C) uncertainty of the temperature measurement, Dobson's original uncertainty analysis is validated. Since the measurements of the present data lie in the same range as that of Dobson's data, this validation can be stated with confidence.

From the results of Dobson's (1994) analysis, the uncertainty of the heat transfer coefficient is on the order of 10%. As previously stated, the uncertainty of the quality is on the order of 2%.

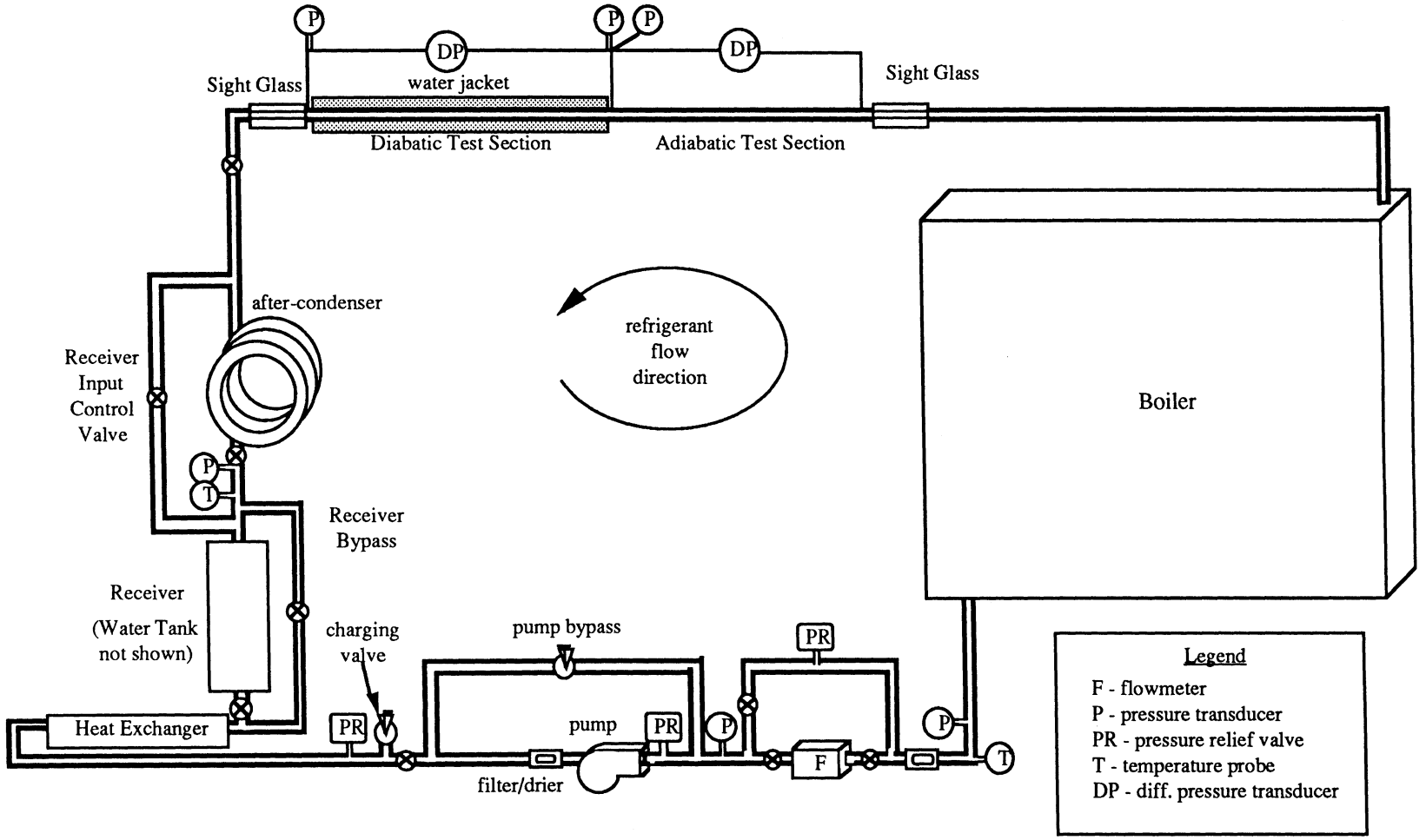

Figure 3.1 Schematic of the Condensation Test Facility

CHAPTER 4

Experimental Results

This chapter presents the experimental results from the data collected testing the ternary zeotrope, R-32/R-125/R-134a (23%/25%/52%). To restate, the tests are run at a condensing temperature of 95°F (35°C) within a 0.277 in (7.04 mm) smooth, horizontal tube. Since the wavy flow regime is temperature difference dependent, the temperature difference between the refrigerant and wall was held constant at approximately 5.4°F (3°C).

Heat fluxes for test conditions varied with mass flux and quality; the increase of both variables increased the heat flux. At a mass flux of 474 klb/ft^2-hr (650 kg/m^2-s), the range of heat flux was 3100 to 7900 Btu/hr-ft^2 (10 to 25 kW/m^2), and at a mass flux of 55 klb/ft^2-hr (75 kg/m^2-s), the range of heat flux was 730 to 2000 Btu/hr-ft^2 (2.3 to 6.2 kW/m^2).

First, the fluid's heat transfer characteristics are analyzed. Experimental heat transfer coefficients are graphed versus quality to give absolute values. Second, the experimental data are compared to Dobson's (1994) predictive correlations by graphing the predicted Nusselt numbers with respect to the experimentally determined Nusselt numbers. Third, the refrigerant's pressure drop data are examined with a graphed comparison to the Souza (1992) correlation. Raw data are tabulated and included in Appendix B.

4.1 Heat Transfer Coefficients

The heart of the results is Figure 4.1. This graph shows local heat transfer coefficients versus average quality at all of the tested mass fluxes. At all but the lower qualities, the trends compare well with previous refrigerant data [Dobson (1994)]. Mass flux and quality continue to exert similar effects on the heat transfer coefficient. Because the area affects the pressure drop and the heat transfer coefficient, the data presents mass flux as opposed to mass flow.

At all mass fluxes, there is a quality dependence on the heat transfer coefficient; as quality increases, the heat transfer coefficient increases monotonically. The slope of this relation increases sharply at qualities below 20%. This effect can be clearly seen at the mass fluxes of 55, 110, and 474 klb/ft^2-hr (75, 150, 650 kg/m^2-s). Interestingly, pure and azeotropic refrigerant data did not show this trend, and at low qualities and mass fluxes, the heat transfer coefficient becomes almost quality independent approaching a single value.

Mass flux has two interesting effects on the heat transfer coefficient. First, as mass flux increases, the slope of the monotonic quality dependence increases. Second, the magnitude of the heat transfer coefficient increases with increasing mass flux. With the first two doublings of mass flux from 55 klb/ft^2-hr (75 kg/m^2-s) to 110 klb/ft^2-hr (150 kg/m^2-s) and again to 220 klb/ft^2-hr (300 kg/m^2-s), the heat transfer coefficient increases moderately. As mass flux increases to 364 klb/ft^2-hr (500 kg/m^2-s) and 474 klb/ft^2-hr (650 kg/m^2-s), the increase of the heat transfer coefficient is much more dramatic. All of these effects are the direct result of the flow regime transition from wavy to annular flow.

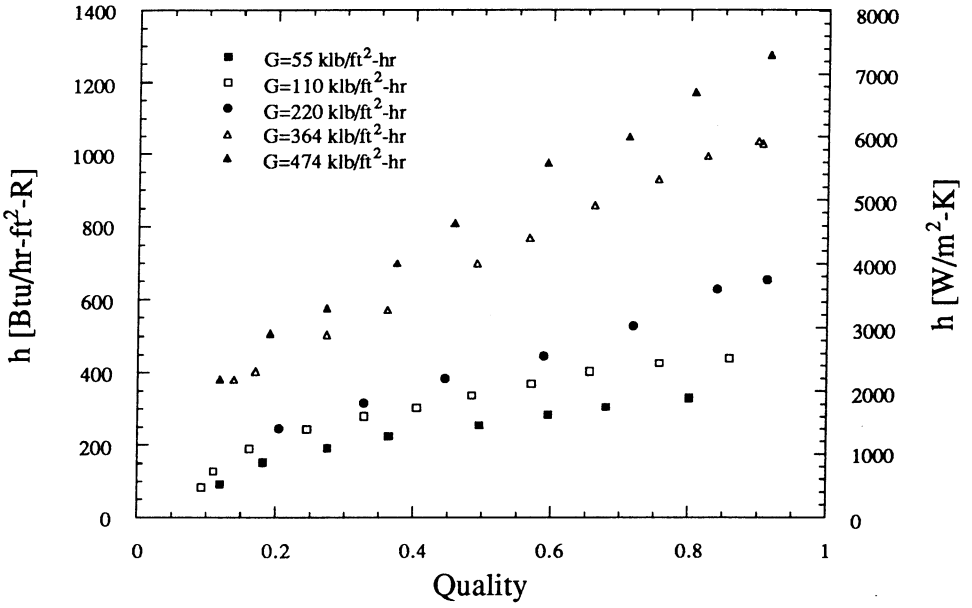

Figure 4.1 Heat transfer coefficient versus average quality

4.2 Results Compared to Correlations

Since the Dobson correlations are our most recently developed heat transfer predictors, they are compared to the data. The Nusselt numbers are graphed as predicted versus experimental values. Figures 4.2 and 4.3 show that the annular flow correlation consistently overpredicts the zeotrope for 474 and 364 klb/ft^2-hr (650 and 500 kg/m^2-s), respectively. This overprediction is a minimum of 15% and as much as 33^1/$_3$%; however, it appears to be consistent through the entire quality range. These results confirm the suspicions of many engineers that the interactions among the refrigerant components degrade the heat transfer coefficient.

Since the data shows linear trends, a simple correction factor is determined for the annular correlation using a least squares curve-fit for both mass fluxes, 474 and 364 klb/ft^2-hr (650 and 500 kg/m^2-s). In Figures 4.4 and 4.5, the correlations are corrected by a multiplier value of 0.836. Thus, the Dobson correlation becomes Equation (4.1):

$$Nu = 0.0192\,Re_l^{0.8}\,Pr_l^{0.4}\left[1+\frac{2.22}{X_{tt}^{0.889}}\right] \qquad (4.1)$$

This correction slightly overpredicts at the higher mass flux. With data from other zeotropic refrigerants, a more sophisticated correction factor might include a mass flux dependence, a compositional dependence, and a dependence due to component interactions. However, these initial data combined with a review of related literature suggest that the correction factor will always be less than unity.

In Figure 4.6, the annular flow correlation continues to overpredict the heat transfer coefficient for G=220 klb/ft^2-hr (300 kg/m^2-s). As the flow approaches the wavy regime, the overprediction of the annular correlation worsens to as much as 40% while the wavy correlation overpredicts by as much as 85%. As described earlier, the sharp degradation of the heat transfer coefficient at low qualities is shown with respect to a correlation based on pure and azeotropic refrigerants. Figure 4.7 shows the Froude number boundary set by Dobson (1994) that separates the wavy and annular flow regimes which is described in Chapter 2.

For the mass flux of 110 klb/ft^2-hr (150 kg/m^2-s), Figure 4.9 shows that the entire quality range lies in the range of the wavy correlation; the Froude number is less than 20 everywhere. As shown in Figure 4.8, the wavy flow correlation again shows the heat transfer degradation at low qualities that is also found at G=220 klb/ft^2-hr (300 kg/m^2-s). Figure 4.10 graphs the wavy correlation predicted Nusselt number versus the experimental Nusselt number for the lowest tested mass flux, 55 klb/ft^2-hr (75 kg/m^2-s). Although the results show disappointingly low heat transfer coefficients, the trend is consistent throughout the wavy flow regime.

4.3 Frictional Pressure Drop

The frictional pressure gradient data for mass fluxes 474 klb/ft^2-hr (650 kg/m^2-s), 364 klb/ft^2-hr (500 kg/m^2-s), and 220 klb/ft^2-hr (300 kg/m^2-s) are presented in Figures 4.12, 4.13, and 4.14, respectively. Data for 110 klb/ft^2-hr (150 kg/m^2-s) and 55 klb/ft^2-hr (75 kg/m^2-s) are not included, because the values approach the uncertainty of the differential pressure transducers. The figures also compare the data to the Souza correlation, and each follows the same trends. Except at the highest quality, the correlation

predicts higher pressure drop than experimentally measured. Also, the predictor possesses a higher slope in its relation to quality, again except for high qualities. Interestingly, at each of the highest qualities the correlation predicts correctly. In all of the reported mass fluxes, at the highest qualities there is a slight decrease in the slope of the relation between the pressure gradient and quality. A similar but much more pronounced phenomenon was observed in Souza's (1992) evaporation research and is attributed to the thinning of the annular film layer, and even to dryout of the wall. This, of course, does not occur in condensation.

At 220 klb/ft^2-hr (300 kg/m^2-s), as shown in Figure 4.14, the pressure drop reaches zero at a quality approximately of 23%. This result is indicative of a complete transition to the wavy flow regime with negligible pressure drop. It is important to point out that the heat transfer mechanism of wavy flow is conduction-based not pressure drop (i.e. vapor shear) based. At the higher mass fluxes, annular flow dominates. Its mechanism for heat transfer sacrifices increased pressure drop for increased heat transfer coefficient. Therefore, the same trends appear in the pressure drop data as in the heat transfer data. Pressure gradient increases monotonically with quality; the slope of this relation increases with mass flux; and the magnitude of the pressure drop increases with increasing mass flux.

Since Dobson's wavy flow correlation uses Souza's pressure drop correlation in its derivation of the forced convection term, one could speculate that if a less overpredictive pressure drop correlation was used then the wavy flow correlation could be improved.

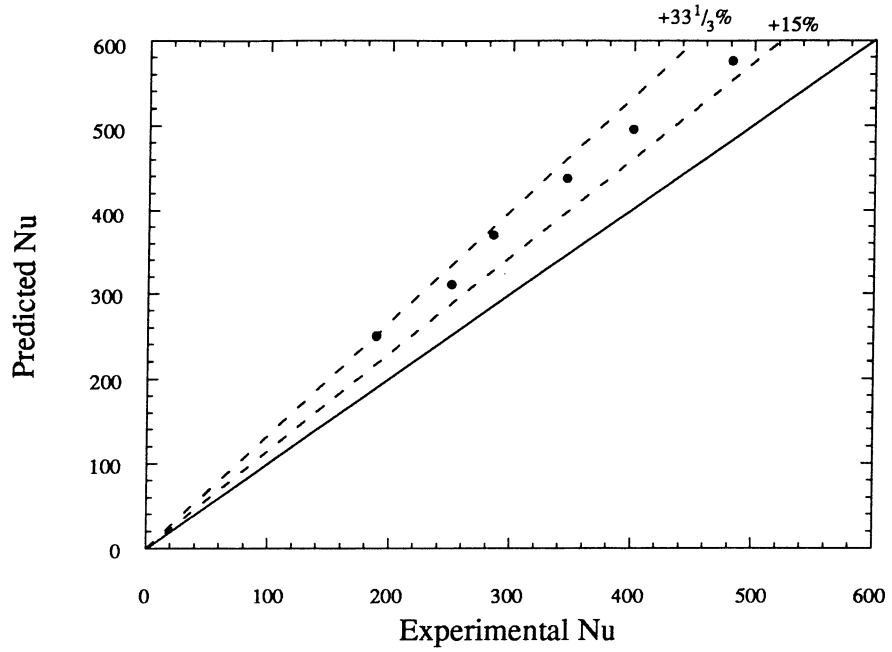

Figure 4.2 Predicted Nusselt number from the annular correlation versus experimental Nusselt number at G=474 klb/ft^2-hr (650 kg/m^2-s)

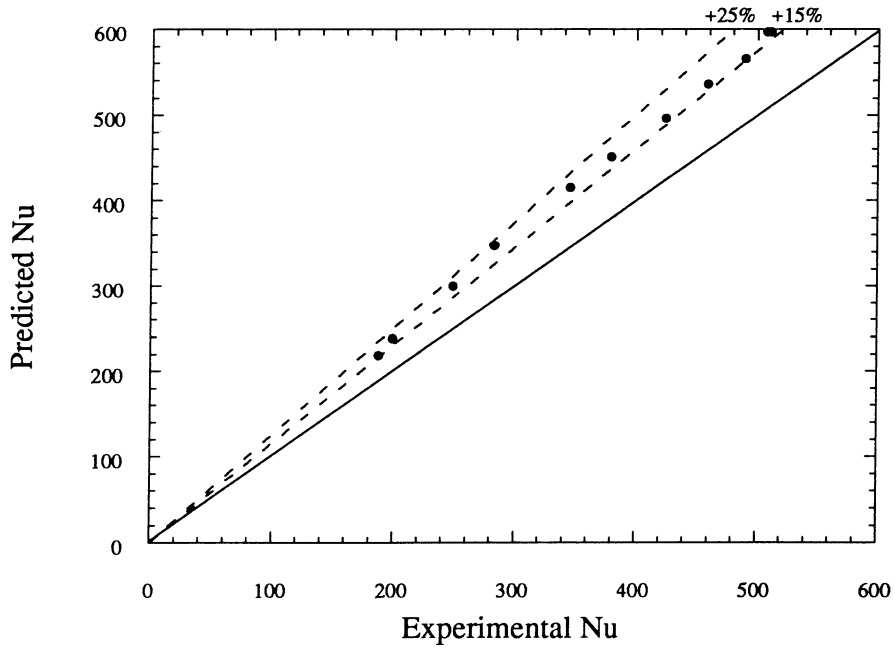

Figure 4.3 Predicted Nusselt number from the annular correlation versus experimental Nusselt number at G=364 klb/ft^2-hr (500 kg/m^2-s)

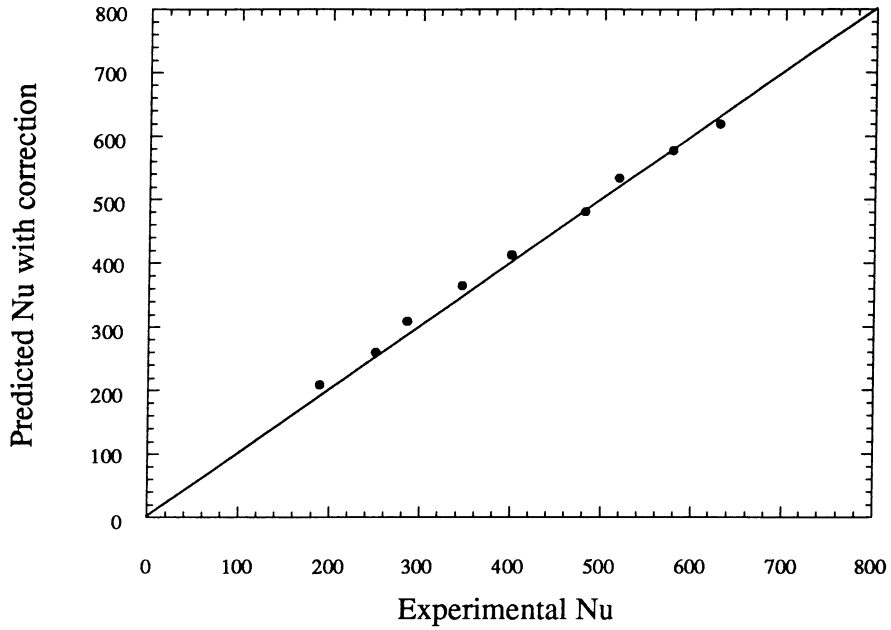

Figure 4.4 Corrected Nusselt number from the annular correlation versus experimental Nusselt number at G=474 klb/ft^2-hr (650 kg/m^2-s)

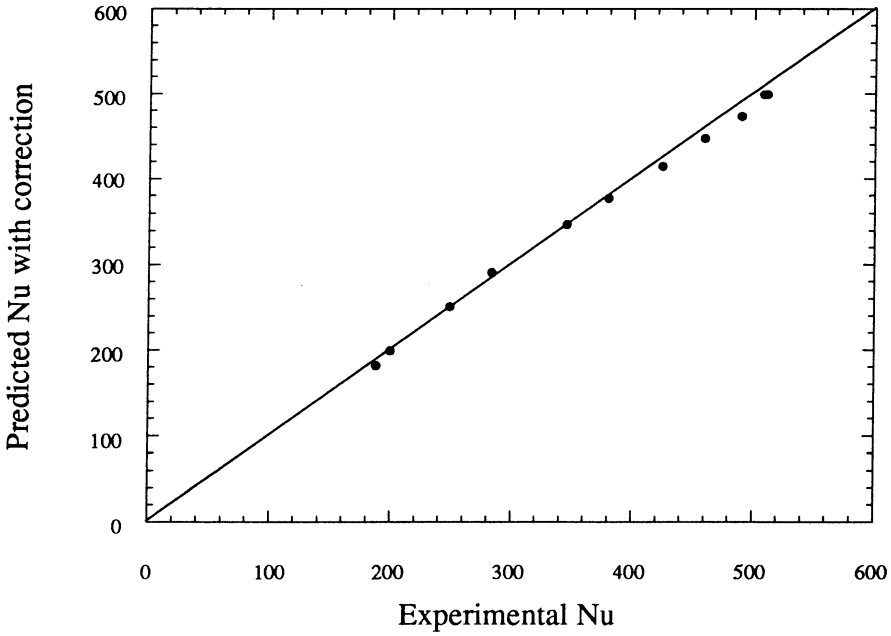

Figure 4.5 Corrected Nusselt number from the annular correlation versus experimental Nusselt number at G=364 klb/ft^2-hr (500 kg/m^2-s)

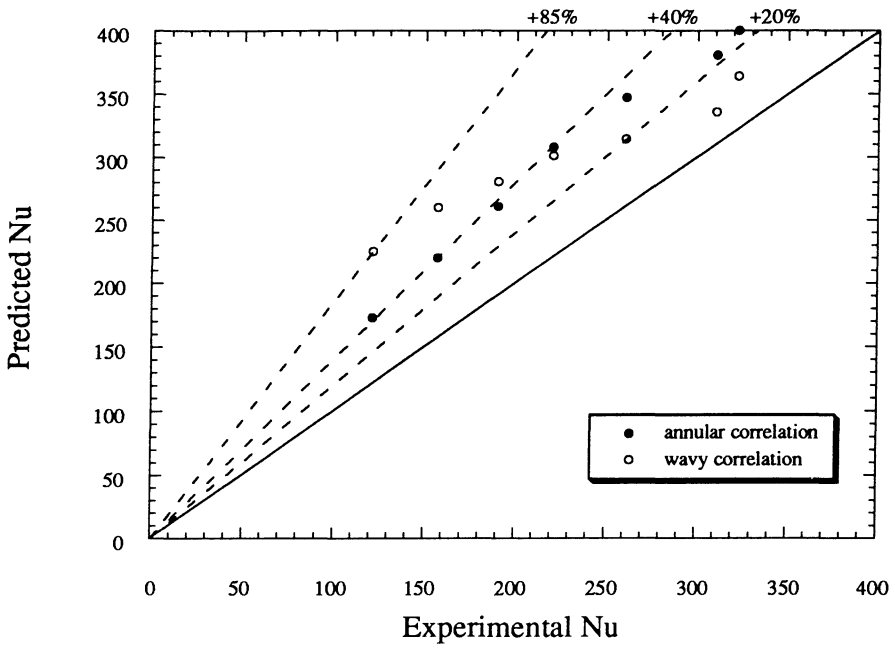

Figure 4.6 Predicted Nusselt number from the annular correlation versus experimental Nusselt number at G=220 klb/ft^2-hr (300 kg/m^2-s)

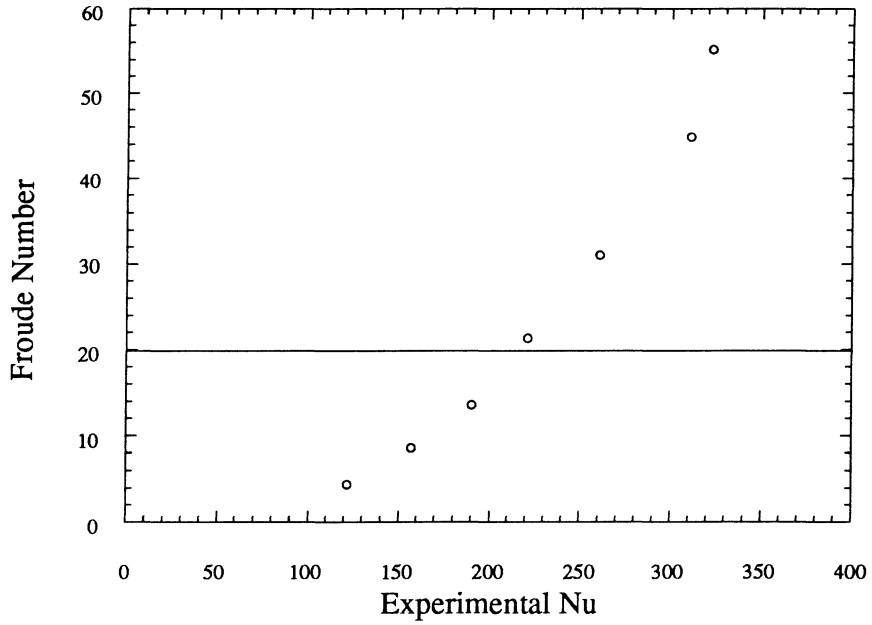

Figure 4.7 Average Froude number versus experimental Nusselt number at G=220 klb/ft^2-hr (300 kg/m^2-s)

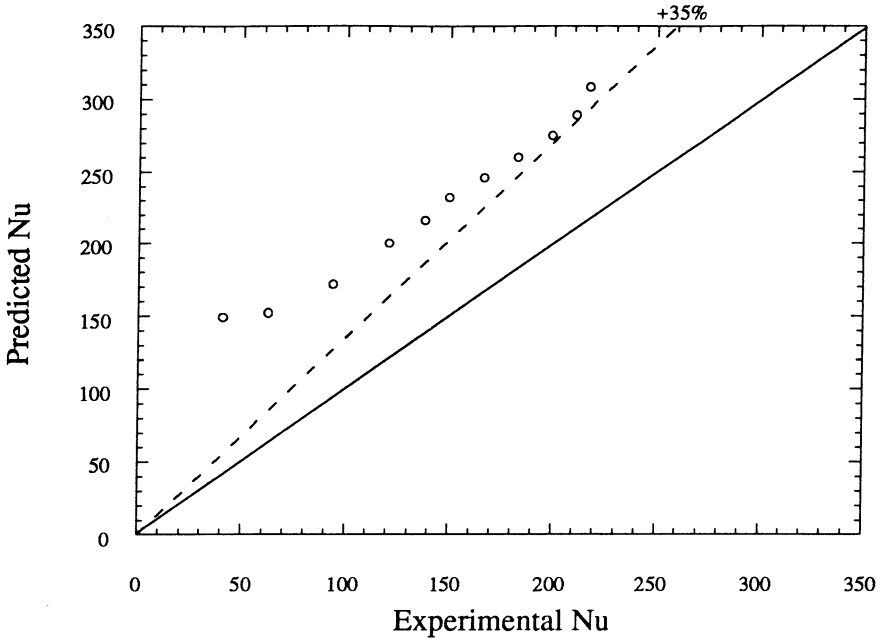

Figure 4.8 Predicted Nusselt number from the wavy correlation versus experimental Nusselt number at G=110 klb/ft^2-hr (150 kg/m^2-s)

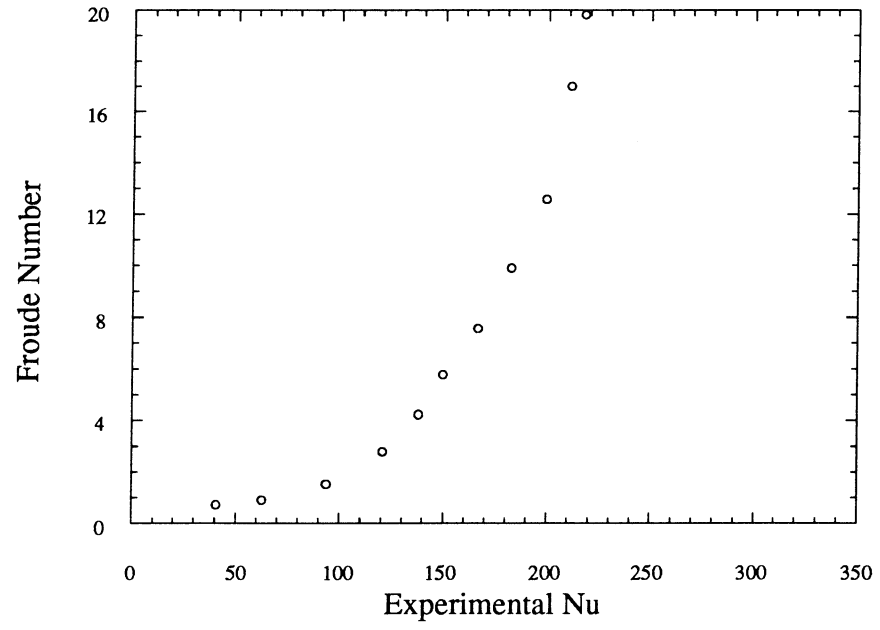

Figure 4.9 Average Froude number versus experimental Nusselt number at G=110 klb/ft^2-hr (150 kg/m^2-s)

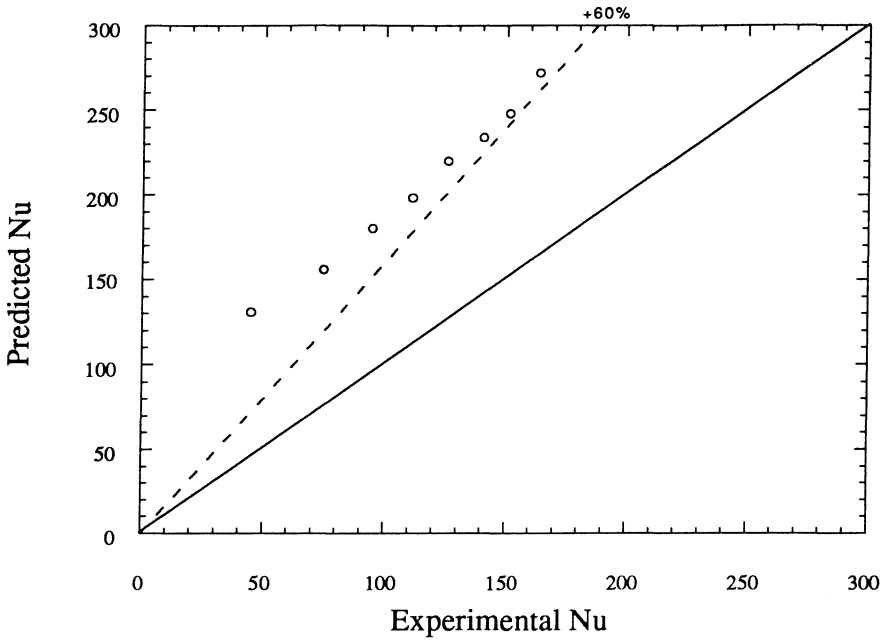

Figure 4.10 Predicted Nusselt number from the wavy correlation versus experimental Nusselt number at G=55 klb/ft^2-hr (75 kg/m^2-s)

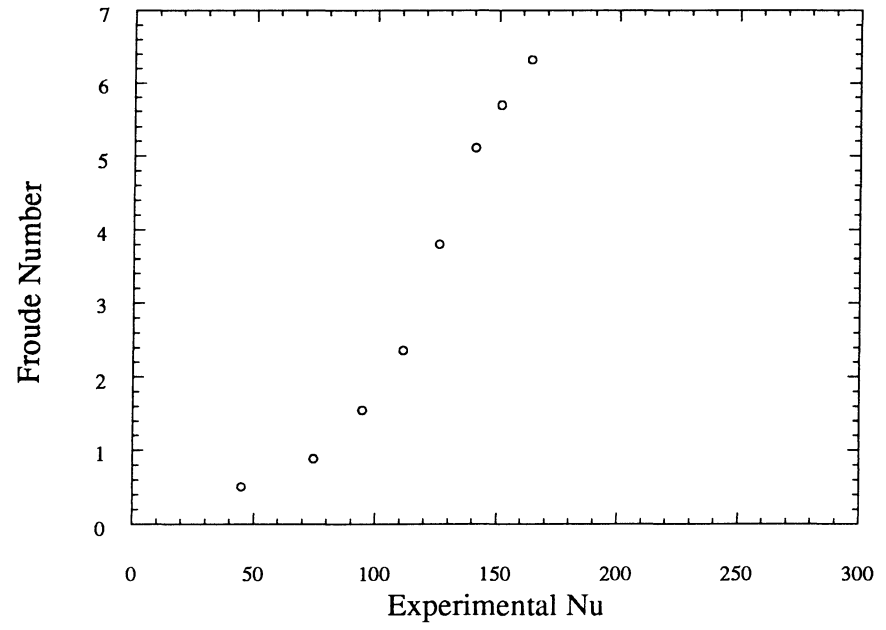

Figure 4.11 Average Froude number versus experimental Nusselt number at G=55 klb/ft^2-hr (75 kg/m^2-s)

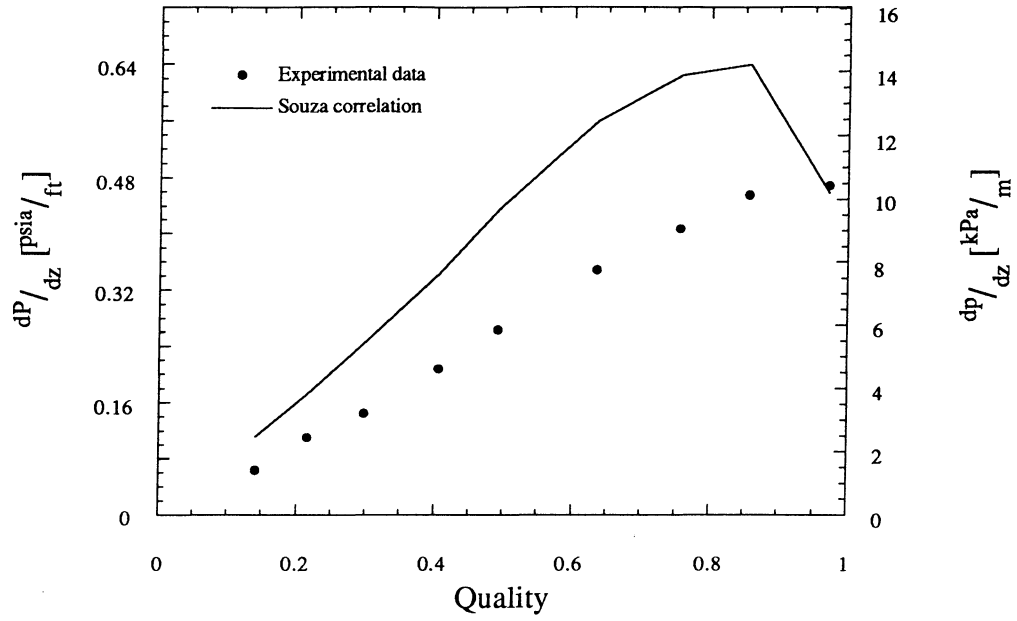

Figure 4.12 Experimental frictional pressure gradient and the Souza correlation versus quality at G=474 klb/ft^2-hr (650 kg/m^2-s)

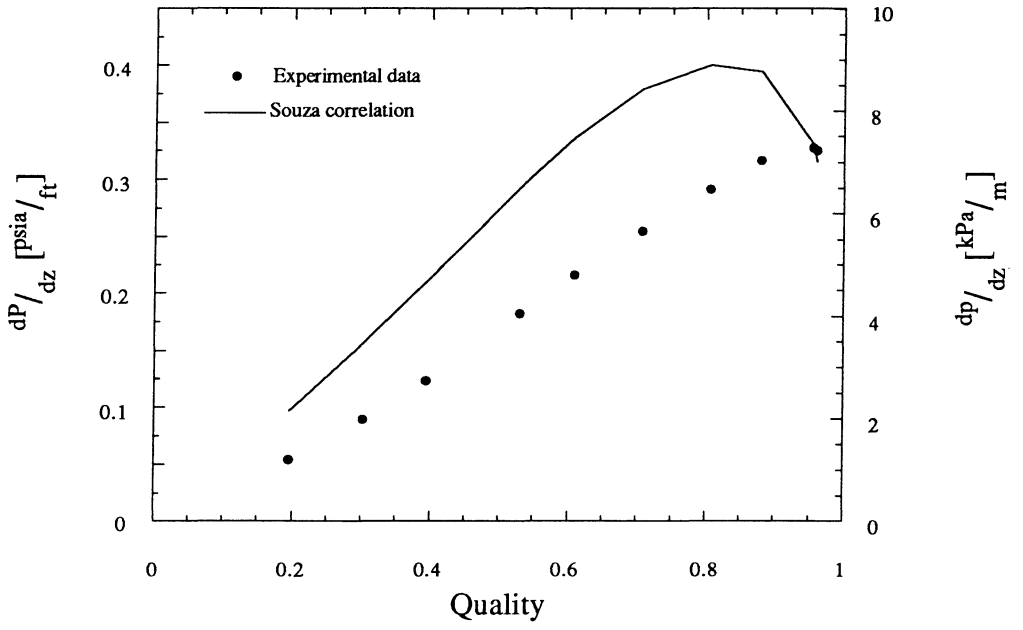

Figure 4.13 Experimental frictional pressure gradient and the Souza correlation versus quality at G=364 klb/ft^2-hr (500 kg/m^2-s)

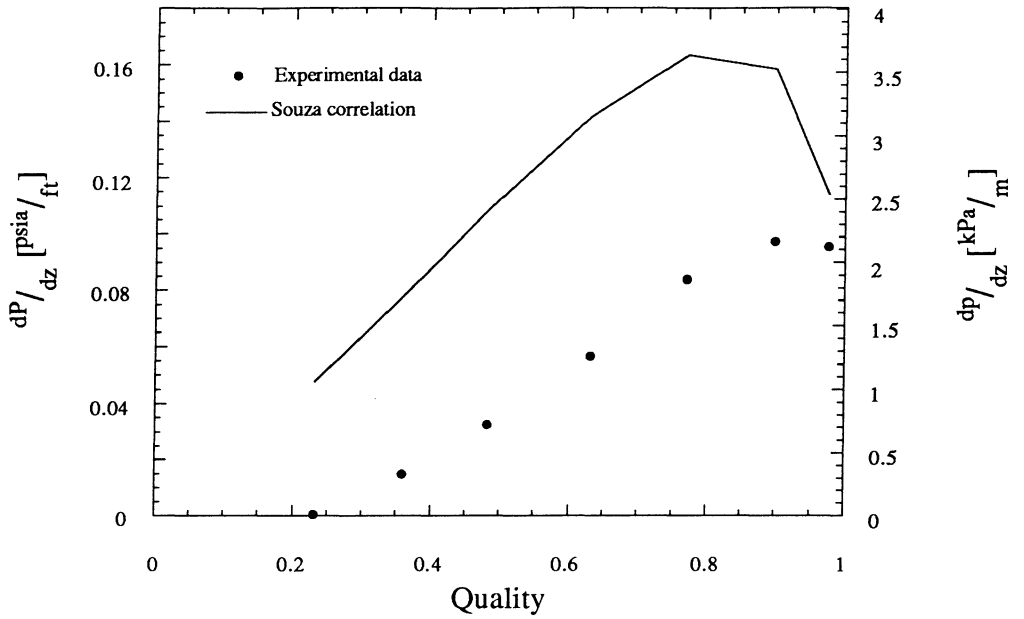

Figure 4.14 Experimental frictional pressure gradient and the Souza correlation versus quality at G=220 klb/ft^2-hr (300 kg/m^2-s)

CHAPTER 5
Conclusions and Recommendations

The purpose of this thesis was to examine the heat transfer of a ternary zeotropic refrigerant mixture condensing in a horizontal tube. To evaluate R-32/R-125/R-134a (23%/25%/52%) as a viable alternative refrigerant, heat transfer coefficients were compared to the Dobson (1994) pure refrigerant correlation. Souza's (1992) correlation of pressure drop was the basis with which the zeotrope's frictional pressure drop was analyzed. This final chapter presents the conclusions from the study and recommendations for future work in this area.

5.1 Conclusions

Degradation in the heat transfer coefficient is found at every data point when compared to the Dobson correlation. At the higher mass fluxes, 364 and 474 klb/ft^2-hr (500 and 650 kg/m^2-s), the zeotrope follows similar mass flux and quality dependencies to that of pure refrigerants; however, Dobson's correlation consistently overpredicts the zeotrope. This relation between the predicted and the experimental Nusselt numbers was curve-fit using the least squares method. A simple correction factor, 0.836, has been included in a modified annular correlation of Dobson. Equation (4.1) can be used to predict this refrigerant's heat transfer coefficient at mass fluxes greater than 364 klb/ft^2-hr (500 kg/m^2-s).

Severe degradation in the heat transfer coefficient is found when the zeotrope approaches the wavy flow regime. Dobson's wavy correlation overpredicts at the lower mass fluxes, 55 and 110 klb/ft^2-hr (75 and 150 kg/m^2-s), and tremendously overpredicts as quality goes to zero. In Dobson's correlation, pure refrigerant heat transfer coefficients approached asymptotically to similar values in the extreme wavy flow regime; however, this zeotrope's heat transfer coefficients continued to decrease.

At the transition mass flux, 220 klb/ft^2-hr (300 kg/m^2-s), between wavy and annular flow, both of the overpredictive results are encountered. The modified annular correlation overpredicts slightly at the high qualities but worsens greatly even before Dobson's Froude number boundary to the wavy flow regime is reached. When the Froude number drops below 20, the wavy correlation actually overpredicts worse than the annular correlation at the same points. However, this result is probably the beginning of the low quality deviation encountered at the lower mass fluxes.

When Souza's frictional pressure drop correlation is applied, the zeotrope is again overpredicted. Two differences to the similar trends that are observed are a slightly higher slope of pressure gradient versus quality curve and an absence of a large decrease in pressure gradient at high qualities. The latter effect is probably due to the fact that the correlation was developed from evaporation data where dryout occurs at high qualities. Of course, dryout does not occur in condensation.

5.2 Recommendations

Even from the literature, the subject of zeotropic heat transfer is largely unresearched. Most investigators, including the author, have curve-fitted the results and have not tested exhaustively to achieve a complete understanding of the effect of component interaction on the mechanisms of heat transfer and pressure drop. In order to develop a generalized heat transfer coefficient predictor for zeotropes akin to Dobson's pure refrigerant correlation, many more zeotropes must be tested. The effects of temperature glide, composition, and departure of the components' properties from the average zeotropic properties, will almost certainly play a role.

Frictional pressure drop within zeotropes can also be explored in parallel with a heat transfer study. Understanding its relation with quality would, at least, offer insight into any differences in the mechanism of heat transfer in forced convection. Also, a zeotropic study should not be restricted to refrigerant mixtures but should span many mixtures. After all, pioneering work to the understanding of two-phase flow regimes was completed with air and water.

REFERENCES

Bivens, D.B. and A. Yokozeki, "Heat Transfer of Refrigerant Mixtures," *Proceedings of the International Refrigeration Conference*, Purdue University, Vol. 1, pp. 141-148, 1992.

Bokhanoviskiy, Yu. G., "Heat Transfer from Freon-12, Freon-22 and Their Mixtures in a Coiled-Tube Condenser," *Heat Transfer-Soviet Research*, Vol. 12, pp. 43-45, 1980.

Bonhomme, D.M., "Condensation of Ozone-Safe Refrigerants in Horizontal Tubes: Experimental Test Facility and Preliminary Results," Master's Thesis, Department of Mechanical and Industrial Engineering, University of Illinois at Urbana-Champaign, 1991.

Cavallini, A. and R. Zecchin, "A Dimensionless Correlation for Heat Transfer in Forced Convective Condensation," *Proceedings of the Fifth International Heat Transfer Conference*, Japan Society of Mechanical Engineers, Vol. 3, pp. 309-313, 1974.

Chato, J.C., "Laminar Condensation inside Horizontal and Inclined Tubes," *ASHRAE Journal*, Vol. 4, pp. 52-60, 1962.

Dhir, V. and J. Lienhard, " Laminar Film Condensation on Plane and Axisymmetric Bodies in Nonuniform Gravity," *Journal of Heat Transfer*, Vol. 93, pp. 97-100, 1971.

Dobson, M.K., "Heat Transfer and Flow Regimes During Condensation in a Horizontal Tube," Doctoral Thesis, Department of Mechanical and Industrial Engineering, University of Illinois at Urbana-Champaign, 1994.

Dobson, M.K., "Initial Condensation Comparison of R-22 with R-134a and R-32/R-125," ACRC Technical Report 41, 1993.

Eckels, S.J. and M.B. Pate, "Evaporation and Condensation Heat Transfer Coefficients for an HCFC-124/HCFC-22/HCFC-152a Blend and CFC-12," *Proceedings of the USNC/IIR and ASHRAE-CFC Conference*, Purdue University, 1991.

Fugii, T. and T. Nagata, "Condensation of Vapor in a Horizontal Tube," *Report of Research Institute of Industrial Science Kyushu University*, Vol. 52, pp. 35-50, 1973.

Gaibel, J.A., "Condensation of a 50/50 Blend of R-32/R-125 in Horizontal Tubes with and without oil," Master's Thesis, Department of Mechanical and Industrial Engineering, University of Illinois at Urbana-Champaign, 1994.

Hinde, D.K., M.K. Dobson, J.C. Chato, M.E. Mainland, and N.L. Rhines, "Condensation of R-134a with and without oils," ACRC Technical Report 26, 1992.

Incropera, F.P. and D.P. DeWitt, *Fundamentals of Heat and Mass Transfer*, 3rd edition, Wiley, New York, 1990.

Inoue, T. et al., "Condensation of Zeotropic Binary Mixtures in a Horizontal Tube (R-113/R-114)," *Proceedings of the Twenty-fifth Japanese National Heat Transfer Symposium*, pp. 460-462, 1988.

Jaster, H. and P.G. Kosky, "Condensation in a Mixed Flow Regime," *International Journal of Heat and Mass Transfer*, Vol. 19, pp. 95-99, 1976.

Koyama, S. et al., "Condensation of Refrigerant Mixtures R-22 + R-114 Inside a Horizontal Tube," *Transactions of the Japan Society of Mechanical Engineers (B)*, Vol. 54(6), pp. 1447-1452, 1988.

Lockhart, R.W. and R.C. Martinelli, "Proposed Correlation of Data for Isothermal, Two-Phase, Two-Component Flow in Pipes," *Chemical Engineering Progress*, Vol. 45(1), pp. 39-48, 1947.

Mochizuki, S. et al., "Condensation of Zeotropic Binary Mixtures in a Horizontal Tube," *Scientific Achievement Reports on Phase Change in Multicomponent Systems*, Japan, pp. 64-65, 1988.

Mochizuki, S. and M. Tominaga, "Condensation Heat Transfer of Zeotropic Binary Mixture (R-113/R-11) inside Horizontal Tubes," *Heat Transfer-Japanese Research*, Vol. 19(2), pp. 33-42, 1990.

Moffat, R.J., "Describing the Uncertainties in Experimental Results," *Experimental Thermal and Fluid Science*, Vol. 1, pp. 3-17, 1988.

Nusselt, W., "Die Oberflachenkondensation des Wasserdampfes," *Z. Vereins Deutscher Ininuere*, Vol. 60, pp. 541-575, 1916.

Rosson, H.F. and J.A. Meyers, "Point Values of Condensing Film Coefficients inside a Horizontal Tube," *Chemical Engineering Progress Symposium Series*, Vol. 61(59), pp. 190-199, 1965.

Soliman, M., J.R. Schuster, and P.J. Berenson, "A General Heat Transfer Correlation for Annular Flow Condensation," *Journal of Heat Transfer*, Vol. 90, pp. 267-276, 1968.

Souza, A.M., J.C. Chato, and J.P. Wattelet, "Pressure Drop during Two-Phase Flow of Refrigerants in Horizontal Smooth Tubes," ACRC Technical Report 25, 1992.

Stoecker, W.F. and E. Kornota, "Condensing Coefficients when using Refrigerant Mixtures," *ASHRAE Transactions*, Vol. 91(2B), pp. 1531-1567, 1985.

Taitel, Y. and A.E. Dukler, "A Model for Predicting Flow Regime Transitions in Horizontal and Near Horizontal Gas-Liquid Flow," *American Institute of Chemical Engineering Journal*, Vol. 22(1), pp. 47-45, 1976.

Traviss, D.P., W.M. Rohsenow, and A.B. Baron, "Forced Convective Condensation in Tubes: A Heat Transfer Correlation for Condenser Design," *ASHRAE Transactions*, Vol. 79(1), pp. 157-165, 1973.

Wang, S-P. and J.C. Chato, "Review of Recent Research on Boiling and Condensation Heat Transfer with Mixtures," ACRC Technical Report 23, 1992.

Wattelet, J.P., "Heat Transfer Flow Regimes of Refrigerants in a Horizontal Tube Evaporator," Doctoral Thesis, Department of Mechanical and Industrial Engineering, University of Illinois at Urbana-Champaign, 1994.

Zivi, S.M., "Estimation of Steady-State Stream Void-Fraction by Means of the Principle of Minimum Entropy Production," *Journal of Heat Transfer*, Vol. 86, pp. 247-252, 1964.

APPENDIX A

Thermophysical Properties

The preferred source of properties is a refrigerant manufacturer. Dr. Don Bivens at DuPont provided tabulated data of R-32/R-125/R-134a (23%/25%/52%) which included relations of temperature, pressure, density, and enthalpies at conditions of saturated liquid and vapor. Transport properties were determined using an interactive program developed by the National Institute of Standards and Technology known as *Refprops*, version 3.X. These tabulated data were curve-fit using fourth order polynomials based on pressure due to the zeotropic temperature glide. Since the original results were calculated in S.I. units, this is how they are presented.

Table A.1 Curve fits of thermophysical properties of R-32/R-125/R-134a (23%/25%/52%)

Property	Curve fit based on pressure [kPa]
T_{liq} [°K]	= 233.59653881 + 0.090019108354P - 4.1171120828e-5P^2 + 1.1164214058e-8P^3 - 1.1946143114e-12P^4
T_{vap} [°K]	= 237.55693121 + 0.098419629569P - 5.1344909261e-5P^2 + 1.5509539418e-8P^3 - 1.8334526012e-12P^4
h_f [kJ/kg]	= 145.05930236 + 0.12157800521P - 4.9866198181e-5P^2 + 1.3511631645e-8P^3 - 1.4021482279e-12P^4
h_{fg} [kJ/kg]	= 242.80480921 - 0.074341109344P + 2.7310061011e-5P^2 - 8.4303001831e-9P^3 + 9.219118354e-13P^4
ρ_f [kg/m^3]	= 1379.3455104 - 0.32546677649P + 1.3727106785e-4P^2 - 3.7205799783e-8P^3 + 3.769505298e-12P^4
ρ_g [kg/m^3]	= 1.1030891419 + 0.038434805267P + 2.0603748962e-6P^2 + 8.4806393427e-11P^3 + 1.8510142788e-13P^4
c_{pl} [kJ/kg-K]	= 1.1822337055 + 1.3918390462e-4P - 4.7387389675P^2 + 1.4632422277e-11P^3 - 1.3333682013e-15P^4
c_{pv} [kJ/kg-K]	= 0.72766706115 + 2.7339392623e-4P - 6.6532052864e-8P^2 + 2.402720122e-11P^3 - 1.5995298974e-15P^4
k_l [W/m-K]	= 0.12834054086 - 5.6360877577e-5P + 2.3999415781e-8P^2 - 6.2660822099e-12P^3 + 6.5098210646e-16P^4
k_v [W/m-K]	= 8.71426145e-3 + 5.2928250666e-6P - 2.3541006186e-9P^2 + 6.1875560523e-13P^3 - 6.0294389287e-17P^4
μ_l [Pa-s *10^{-7}]	= 3950.4188748 - 3.3798653731P + 1.9055612995e-3P^2 - 5.3962677824e-7P^3 + 5.7698262205e-11P^4
μ_v [Pa-s *10^{-7}]	= 98.678791681 + 0.03885792107P - 1.4419678508e-5P^2 + 4.2223084508e-9P^3 - 3.7776073406e-13P^4

APPENDIX B

Experimental Data

Table B.1 Heat transfer data for G=55 klb/ft^2-hr (75 kg/m^2-s)

G [kg/m^2-s]	x_{avg} [%]	Δx [%]	P_{sat} [kPa]	h [W/m^2-K]	Nu_{exp}	Nu_{pred}	flow regime
74.8	80.1	24.8	1425.0	1890	164	272	wavy-annular
73.9	68.0	23.3	1418.7	1750	151	248	wavy-annular
74.4	59.6	22.1	1418.7	1626	141	234	wavy
75.1	49.6	19.4	1418.7	1458	126	220	wavy
75.4	36.4	17.7	1421.9	1287	111	198	wavy
74.4	27.5	15.2	1421.8	1093	95	180	wavy
75.8	18.2	12.6	1406.0	867	75	156	wavy
76.3	12.0	8.9	1391.8	523	45	131	wavy

Table B.2 Heat transfer data for G=110 klb/ft^2-hr (150 kg/m^2-s)

G [kg/m^2-s]	x_{avg} [%]	Δx [%]	P_{sat} [kPa]	h [W/m^2-K]	Nu_{exp}	Nu_{pred}	flow regime
153.1	85.9	15.7	1418.2	2516	218	308	wavy-annular
151.8	75.7	14.9	1417.9	2440	211	289	wavy-annular
149.9	65.6	14.2	1418.2	2305	199	275	wavy-annular
151.0	57.1	13.6	1418.2	2113	182	260	wavy-annular
150.9	48.4	12.7	1419.5	1926	167	246	wavy-annular
152.4	40.4	11.8	1415.6	1731	150	232	wavy
152.1	32.8	11.4	1417.2	1597	138	216	wavy
152.4	24.5	9.7	1417.8	1397	121	200	wavy
149.8	16.2	8.5	1421.8	1083	94	172	wavy
152.6	11.0	5.7	1419.9	725	63	152	wavy
151.1	9.3	3.0	1422.3	472	41	149	wavy

Table B.3 Heat transfer data for G=220 klb/ft^2-hr (300 kg/m^2-s)

G [kg/m^2-s]	x_{avg} [%]	Δx [%]	P_{sat} [kPa]	h [W/m^2-K]	Nu_{exp}	Nu_{pred}	flow regime
300.1	91.3	12.9	1415.8	3735	323	400	annular
300.4	84.1	11.6	1418.5	3589	310	381	annular
300.6	71.9	10.4	1418.0	3017	261	347	wavy-annular
300.3	58.9	8.3	1422.6	2553	221	308	wavy-annular
299.9	44.6	7.3	1420.8	2199	190	281	wavy-annular
300.1	32.8	6.0	1423.1	1812	157	260	wavy-annular
300.5	20.5	5.2	1424.9	1406	122	225	wavy

Table B.4 Heat transfer data for G=364 klb/ft^2-hr (500 kg/m^2-s)

G [kg/m^2-s]	x_{avg} [%]	Δx [%]	P_{sat} [kPa]	h [W/m^2-K]	Nu_{exp}	Nu_{pred}	flow regime
497.5	90.5	11.2	1416.6	5881	508	597	annular
500.3	89.9	11.3	1416.1	5915	511	597	annular
499.6	82.5	11.0	1416.1	5675	490	566	annular
499.1	75.4	10.3	1419.6	5312	459	536	annular
500.3	66.1	9.4	1420.6	4909	425	496	annular
500.1	56.7	8.5	1416.7	4396	380	451	annular
500.1	49.1	7.9	1418.5	3998	346	415	wavy-annular
499.4	36.1	6.6	1426.9	3271	283	348	wavy-annular
500.4	27.3	6.0	1418.3	2878	249	300	wavy-annular
498.7	17.0	5.1	1416.9	2309	200	238	wavy-annular
501.7	13.9	4.9	1412.4	2176	189	218	wavy

Table B.5 Heat transfer data for G=474 klb/ft^2-hr (650 kg/m^2-s)

G [kg/m^2-s]	x_{avg} [%]	Δx [%]	P_{sat} [kPa]	h [W/m^2-K]	Nu_{exp}	Nu_{pred}	flow regime
646.8	91.6	11.3	1413.5	7287	629	742	annular
652.0	80.7	10.0	1410.5	6692	578	692	annular
651.0	71.1	9.0	1418.9	5991	518	639	annular
654.2	59.3	8.3	1412.0	5577	481	576	annular
655.4	45.8	6.7	1418.0	4627	400	495	annular
646.9	37.4	6.3	1416.9	4000	346	437	annular
649.2	27.3	5.1	1418.2	3298	285	370	wavy-annular
651.3	19.1	4.9	1415.0	2900	251	311	wavy-annular
646.8	11.9	4.5	1414.4	2184	189	250	wavy-annular